COBEM 99
XV Congresso Brasileiro de Engenharia Mecânica
15th Brazilian Congress of Mechanical Engineering
22 - 26 de Novembro de 1999 / November 22 - 26, 1999 Águas de Lindóia, São Paulo,

A NUMERICAL STUDY OF TWO-PHASE FLOWS IN AXISYMMETRIC SOLID ROCKET MOTOR NOZZLES

Marcos A. Novo
Mectron E.I.C. Ltda, Aeronautical Systems Division
Av. Nove de Julho, 1027 - 703 Jd. Apolo
12243-200 - São José dos Campos, SP, Brazil
João L. F. Azevedo
Rubens P. da Silva
Shailon I. A. Menezes
Centro Técnico Aeroespacial, Instituto de Aeronáutica e Espaço
CTA/IAE/ASE-N, Praça Mal. Eduardo Gomes, 50, Vila das Acácias
12228-904 - São José dos Campos, SP, Brazil

Abstract. *Aluminum oxide particles present in the flow in solid rocket motor nozzles contribute to the loss of thrust as momentum is transfered from the gas phase to the particles. A tool capable of simulating such flows has been developed so as to predict the thrust loss and the behavior of the alumina particles inside the flow. The problem for the gas phase is modeled by the Euler equations augmented with source terms to take the interaction between phases into account. The particles are simulated as a continuum of particles, and the formulation is again very similar to the Euler equations except that there is no counterpart to the pressure. The governing equations are integrated in time by the implicit Euler method in the context of the Beam and Warming approximate factorization scheme. Since the scheme uses central differences, artificial dissipation terms must be added and Pulliam's nonlinear artificial dissipation model was selected. The use of the nonlinear artificial dissipation terms has yielded a much faster convergence rate than simpler artificial dissipation models. A detailed parametric study was performed in order to precisely determine how the solution quality and the convergence rate are affected by the changes in the problem variables.*

Keywords: *Two-phase flows, Axisymmetric flows, Nozzle, Nonlinear artificial dissipation, Euler equations*

1. INTRODUCTION

In recent years, several numerical studies have been performed in order to estimate dynamic characteristics of the gas-particle interaction in two-phase flows. The present study has focused the case of dilute flows which are flows where particle motion is controlled by aerodynamic forces and not by particle collision. Here particle collisions are rare and the information travels along trajectories. This implies in severe restrictions to the definition of a

pressure quantity for the particle phase. Since the information comes to the particles by means of its trajectory, the proximity between a particle and the wall has no direct influence on the particle itself. Moreover, the streamlines of the particles differ from those of the nearby gas because of the inertia. Particle streamlines have a smaller curvature than gas streamlines. This fact leads to a particular phenomenon in nozzles which is the creation of a particle-free region in the divergent part of the nozzle.

In light of the particularities of the two-phase flow, this work is concerned with the implementation of an efficient computational model to simulate the flow along solid rocket motor nozzles. Since solid rocket motors are usually built as axisymmetric volumes, the algorithm uses an axisymmetric formulation. The gas flow is considered inviscid except for its interaction with the particles, leading to an Euler formulation. The governing equations are written in strong conservation-law form for general body conforming curvilinear coordinates. The Beam and Warming (1976, 1978) implicit approximate factorization algorithm is used with implicit Euler time march method and central differences are employed to discretize all spatial derivatives. Attention was paid to the use of an efficient nonlinear artificial dissipation model. In particular, Pulliam's (1986) model was implemented to control the nonlinear instabilities. The quality of the solution greatly improved with this artificial dissipation model, reducing numerical oscillations close to the nozzle wall. The use of the variable time step helped improving the convergence rate, reducing the computational time of the simulations.

2. GOVERNING EQUATIONS AND BOUNDARY CONDITIONS

The problem was modeled based on the work of Ishii et al. (1987, 1989) and Chang (1980, 1990). Nagata (1993) achieved initial results using a two-dimensional formulation and the implementation of the present axisymmetric formulation was performed taking into account the following hypothesis: (a) the flow is in steady state; (b) no phase changes take place; (c) the gas is inviscid except for its interaction with the particles; (d) the gas is a perfect gas with constant composition and constant specific heats; (e) the flow is dilute; (f) there is no mass transfer between phases; (g) particle and gas radiation effects are not considered; (h) no external work is done, nor there is any external heat transfer and the effects of gravity are neglegible; (i) thermal and Brownian motion of the particles are small and were not considered; (j) the particle volume is neglegible and the average distance between particles is small when compared to the smallest dimension in the grid; (k) particles are solid spheres with uniform diameter, constant material density, constant specific heat and uniform internal temperature; (l) the contribution of the solid phase to the system pressure is null; (m) both solid and gas phase are treated as continua.

Considering the hypotheses stated above, the axisymmetric equations for the solid phase are written for a general curvilinear coordinate system. With the use of nondimensional quantities, the equations are written as

$$\frac{\partial \hat{Q}_p}{\partial \tau} + \frac{\partial \hat{E}_p}{\partial \xi} + \frac{\partial \hat{F}_p}{\partial \eta} + \hat{H}_p = 0 \quad ,$$

$$\hat{Q}_p = J^{-1}\begin{Bmatrix} \rho_p \\ \rho_p u_p \\ \rho_p v_p \\ h_p \end{Bmatrix} \quad , \quad \hat{E}_p = J^{-1}\begin{Bmatrix} \rho_p U_p \\ \rho_p u_p U_p \\ \rho_p v_p U_p \\ h_p U_p \end{Bmatrix} \quad , \quad \hat{F}_p = J^{-1}\begin{Bmatrix} \rho_p V_p \\ \rho_p u_p V_p \\ \rho_p v_p V_p \\ h_p V_p \end{Bmatrix} \quad , \qquad (1)$$

where the source term is defined as

$$\hat{H}_p = -J^{-1}\rho_p A_p \begin{Bmatrix} 0 \\ (u-u_p) \\ (v-v_p) \\ B_p \end{Bmatrix} \quad . \qquad (2)$$

In a similar fashion, the axisymmetric equations for the gas phase are written in terms of the vector of conserved variables and the flux vectors as

$$\frac{\partial \hat{Q}}{\partial \tau} + \frac{\partial \hat{E}}{\partial \xi} + \frac{\partial \hat{F}}{\partial \eta} + \hat{H} = 0 \quad ,$$

$$\hat{Q} = J^{-1}\begin{Bmatrix} \rho \\ \rho u \\ \rho v \\ e \end{Bmatrix} \quad , \quad \hat{E} = J^{-1}\begin{Bmatrix} \rho U \\ \rho u U + \xi_x p \\ \rho v U + \xi_y p \\ (e+p)U - \xi_t p \end{Bmatrix} \quad , \quad \hat{F} = J^{-1}\begin{Bmatrix} \rho V \\ \rho u V + \eta_x p \\ \rho v V + \eta_y p \\ (e+p)V - \eta_t p \end{Bmatrix} \quad , \qquad (3)$$

and for the gas phase the source term is defined by the equation

$$\hat{H} = J^{-1}\begin{Bmatrix} 0 \\ \rho_p A_p (u-u_p) \\ \rho_p A_p (v-v_p) - p/R \\ \rho_p A_p B_p \end{Bmatrix} \quad , \qquad (4)$$

All terms use dimensionless quantities as defined in usual CFD applications (see, for instance, Azevedo, 1992 and 1995, and Nagata, 1993). In the previous expressions, some of the quantities which come from the two-phase assumption need some special clarification. The density for the solid phase is defined as

$$\overline{\rho}_p = \frac{\dot{m}}{S \times \rho_0 \times \sqrt{u_p^2 + v_p^2}} \quad , \qquad (5)$$

and the particle drag force is calculated according to Henderson (1976) and Ishii et al. (1987, 1989). Considering the particle as a sphere, the particle frontal area and its velocity relative to the neighboring gas phase lead to an exchange in momentum between the phases. The particle is accelerated by the gas and the gas looses momentum. This fact is described by Eq. (6), where the drag coefficient for the case in sight is written as

$$\frac{1}{2} C_d \pi r_p^2 \rho \left[(u-u_p)^2 \hat{i} + (v-v_p)^2 \hat{j} \right] = m_p \frac{4}{3} \pi r_p^3 \frac{D\vec{V}_p}{Dt} \quad , \quad Cd_{Stokes} = \frac{24}{\mathrm{Re}_p} \quad . \qquad (6)$$

The particle Reynolds, Prantl and Nusselt numbers are given by the equations

$$\mathrm{Re}_p = \frac{2 r_p \rho}{\mu_g}\sqrt{\left(u-u_p\right)^2+\left(v-v_p\right)^2} \quad , \qquad \mathrm{Pr} = \frac{\mu_g C_{pg}}{\kappa} \qquad \text{and}$$
$$Nu = 2 + 0{,}459\,\mathrm{Re}_p^{0{,}55}\,\mathrm{Pr}^{0{,}33} \tag{7}$$

where the local viscosity coefficient for the gas is given by

$$\mu_g = \mu_{g0}\left(\frac{T}{T_0}\right)^{0{,}6} \tag{8}$$

The energy conservation law is achieved by the the heat flux compatibility between phases and is represented by the equation

$$\left(\dot{q}_p\right)_{atrito} = \frac{9\mu_g f_p \rho_p}{2 m_p r_p^2}\left[\left(u-u_p\right)\,u_p + \left(v-v_p\right)\,v_p\,\right] \tag{9}$$

with the momentum and the energy parameters defined as

$$A_p = \frac{9\mu_g f_p}{2 m_p r_p^2 a_*} \qquad \text{and} \quad B_p = \left(\bar{u}-\bar{u}_p\right)\,\bar{u}_p + \left(\bar{v}-\bar{v}_p\right)\,\bar{v}_p - g_c\left(\bar{T}_p - \bar{T}\right) \tag{10}$$

and with the drag and convection parameters written as

$$f_p = \frac{Cd}{Cd_{Stokes}} \qquad \text{and} \quad g_c = \frac{\left(\gamma+1\right)\,Nu}{\left(\gamma-1\right)\,6 f_p\,\mathrm{Pr}} \quad . \tag{11}$$

The effects of radiation of the particles inside the nozzle are not considered here since this effect is small. Particle emissivity coefficients, as shown in the work by Eversole (1984), are seldom documented. In order to calculate the properties of both phases, Eqs. (12) are used for the solid phase,

$$\bar{e}_{i\,p} = \left[\frac{\bar{h}_p}{\bar{\rho}_p} - \frac{1}{2}\left(\bar{u}_p^2+\bar{v}_p^2\right)\right] \quad \text{and} \quad \bar{T}_p = \frac{1}{\omega}\left(\frac{\gamma+1}{\gamma-1}\right)\left[2\frac{\bar{h}_p}{\bar{\rho}_p} - \left(\bar{u}_p^2+\bar{v}_p^2\right)\right] \quad , \tag{12}$$

and Eqs. (13) for the gas phase,

$$\bar{p} = \left(\frac{\gamma+1}{2\gamma}\right)\bar{\rho}\,\bar{T} \quad , \qquad \bar{T} = \frac{2\gamma}{\bar{\rho}}\left(\frac{\gamma-1}{\gamma+1}\right)\left[\bar{e} - \frac{1}{2}\bar{\rho}\left(\bar{u}^2+\bar{v}^2\right)\right] \quad ,$$
$$\bar{e}_i = \left[\frac{\bar{e}}{\bar{\rho}} - \frac{1}{2}\left(\bar{u}^2+\bar{v}^2\right)\right] \quad \text{and} \quad \bar{p} = \left(\gamma-1\right)\left[\bar{e} - \frac{1}{2}\bar{\rho}\left(\bar{u}^2+\bar{v}^2\right)\right] \quad . \tag{13}$$

The stated boundary conditions applied to the problem are as following: (a) The flow is tangent to the wall; (b) Symmetry conditions are applied to the centerline; (c) For the nozzle

inlet one property has its numerical boundary condition imposed by the characteristic one-dimensional relations for the Euler equations and the other three property values are fixed; (d) For the nozzle exit a zeroth-order extrapolation is applied for all conserved variables.

In the nozzle inlet, the flow is subsonic and the fixed properties are the stagnation pressure, temperature and the angle of incidence. The fourth property is obtained by the characteristic relations for "operation" in the x direction (Azevedo et al., 1995). The nozzle exit has two possible conditions. When the flow is subsonic, the static pressure is defined and the other properties are obtained using the x-direction characteristic relations. All four characteristic relations are used when the flow is supersonic at the exit.

As for the boundary conditions of the particle phase, since there is no pressure counterpart for the solid phase, the information is transmitted by means of the particle trajectories. This is the main difference between the phases. In the centerline and on the wall, conditions are set just as previously mentioned for the gas phase. For the nozzle inlet, four conditions must be set: particle mass flux per unit of time, longitudinal and normal velocity components equal to the gas phase and particle temperature identical to the gas temperature. At the nozzle exit, all properties must be extrapolated from the interior since all information is carried along by the particle streamlines, as previously discussed. A detailed discussion of the application of characteristic relations in this case can be found in Novo and Menezes (1998).

3. NUMERICAL ALGORITHM

For the gas phase, the finite difference equations for the axisymmetric case are written as

$$L_\xi \; L_\eta \; \Delta_t \; \hat{Q}^n = R_\xi + R_\eta - \Delta t \; \hat{H}^n \quad . \tag{14}$$

The operators in Eq. (14) are defined in a similar fashion to those in the work of Azevedo et al. (1992, 1995), where a detailed description of the several operators can be found. Here, the operators are written as

$$\begin{aligned} L_\xi &= \left(I + \Delta t \; \delta_\xi A^n - \Delta_t \varepsilon_I J^{-1} \nabla_\xi \Delta_\xi J\right) \quad , \qquad R_\xi = -\Delta t \; \delta_\xi \hat{E}^n + D_\xi \quad , \\ L_\eta &= \left(I + \Delta t \; \delta_\eta B^n - \Delta_t \varepsilon_I J^{-1} \nabla_\eta \Delta_\eta J\right) \quad \text{and} \quad R_\eta = -\Delta t \; \delta_\eta \hat{F}^n + D_\eta \quad . \end{aligned} \tag{15}$$

The inviscid flux Jacobian matrices A and B, which appear in the linearization process through Taylor series expansion, are described in detail by Beam et al. (1975) and by Novo and Menezes (1998), and their expressions will not be repeated here.

In the previous expressions, the artificial dissipation terms necessary for the numerical stability of the algorithm have already been introduced. The explicit, right-hand side artificial dissipation operators, according to Pulliam's (1986) nonlinear model, are given by

$$\begin{aligned} D_{\xi_{i,j}} &= D^{(nl)}_{\xi_{i,j}} = \nabla_\xi \left(\sigma_{i+1,j} J^{-1}_{i+1,j} + \sigma_{i,j} J^{-1}_{i,j}\right)\left(\varepsilon^{(2)}_{\xi_{i,j}} \Delta_\xi J_{i,j} \hat{Q}^n_{i,j} - \varepsilon^{(4)}_{\xi_{i,j}} \Delta_\xi \nabla_\xi \Delta_\xi J_{i,j} \hat{Q}^n_{i,j}\right) \\ D_{\eta_{i,j}} &= D^{(nl)}_{\eta_{i,j}} = \nabla_\eta \left(\sigma_{i,j+1} J^{-1}_{i,j+1} + \sigma_{i,j} J^{-1}_{i,j}\right)\left(\varepsilon^{(2)}_{\eta_{i,j}} \Delta_\eta J_{i,j} \hat{Q}^n_{i,j} - \varepsilon^{(4)}_{\eta_{i,j}} \Delta_\eta \nabla_\eta \Delta_\eta J_{i,j} \hat{Q}^n_{i,j}\right) \end{aligned} \tag{16}$$

where

$$
\begin{aligned}
&\varepsilon^{(2)}_{\xi_{i,j}} = K_2 \Delta t \max\left[\upsilon_{\xi_{i+1,j}}, \upsilon_{\xi_{i,j}}, \upsilon_{\xi_{i-1,j}}\right] \quad , \quad \varepsilon^{(4)}_{\xi_{i,j}} = \max\left[0, \left(K_4 \Delta t - \varepsilon^{(2)}_{\xi_{i,j}}\right)\right] \quad , \\
&\varepsilon^{(2)}_{\eta_{i,j}} = K_2 \Delta t \max\left[\upsilon_{\eta_{i,j+1}}, \upsilon_{\eta_{i,j}}, \upsilon_{\eta_{i,j-1}}\right] \quad , \quad \varepsilon^{(4)}_{\eta_{i,j}} = \max\left[0, \left(K_4 \Delta t - \varepsilon^{(2)}_{\eta_{i,j}}\right)\right] \quad , \\
&\upsilon_{\xi_{i,j}} = \frac{\left|p_{i+1,j} - 2p_{i,j} + p_{i-1,j}\right|}{\left(p_{i+1,j} + 2p_{i,j} + p_{i-1,j}\right)} \quad , \quad \upsilon_{\eta_{i,j}} = \frac{\left|p_{i,j+1} - 2p_{i,j} + p_{i,j-1}\right|}{\left(p_{i,j+1} + 2p_{i,j} + p_{i,j-1}\right)} \quad , \\
&\sigma_{i,j} = \left(|U| + a\sqrt{\xi_x^2 + \xi_y^2} + |V| + a\sqrt{\eta_x^2 + \eta_y^2}\right)_{i,j} \quad .
\end{aligned}
\tag{17}
$$

At points adjacent to the computational boundaries, the fourth order artificial dissipation terms used in the model are reduced to second order terms similar to those used in the left-hand side operators. Hence,

$$
D_\xi = -\Delta_t \varepsilon_E J^{-1} \nabla_\xi \Delta_\xi J \hat{Q}^n \quad , \quad D_\eta = -\Delta_t \varepsilon_E J^{-1} \nabla_\eta \Delta_\eta J \hat{Q}^n \quad . \tag{18}
$$

The algorithm for the solid phase is equivalent to the one presented above for the gas phase, except for the flux Jacobian matrices A and B, as described in Novo and Menezes (1998). Moreover, the explicit operator in the ξ-direction is simply written as

$$
R_\xi = -\Delta t \nabla_\xi \hat{E}_p^{\,n} \quad . \tag{19}
$$

The reader should observe that Eq. (19) is conceptually correct because the “solid phase flow” should not see downstream information. This is achieved by backward differencing the spatial derivatives in the direction essentially aligned with the flow. Another important procedure applied to the model was the use of a variable time step throughout the flowfield. Hence, the CFL number was kept constant and the time step had its value determined by the characteristic velocity of information propagation in the flow. Convergence was achieved in nearly 6000 iterations while, in the constant time step case, it required 150000 iterations, as shown by Novo and Menezes (1998). Selection of the variable time step option reduces computational efforts, leading to a 20 times faster convergence. This method is represented by

$$
\Delta t_{i,j} = \frac{CFL}{c_{i,j}} \tag{20}
$$

where the characteristic velocity of propagation of information in the flow is

$$
c_{i,j} = máx\left(|U| + a\sqrt{\xi_x^2 + \xi_y^2}, |V| + a\sqrt{\eta_x^2 + \eta_y^2}\right)_{i,j} \tag{21}
$$

4. NUMERICAL RESULTS

Validation of this code was performed by comparing computational results with experimental and computational data presented by Mehta and Jayachandran (1998), Ishii et al. (1987) and by Chang (1980). These comparisons, presented by Novo and Menezes (1998), aimed at demonstrating the physical results of the code. The following conditions where applied to the model: T_0 = 3200 K; Pr = 0.7; ρ_0 = 1,0 kg/m^3; δ = 0.6; C_{pg} = 1034 J/kg.K; C_{pp} = 1686 J/kg.K; γ = 1.4; ρ_p = 3,99 x 10^3 kg/m^3; and μ = 7,974 x 10^{-5} kg/s.m.

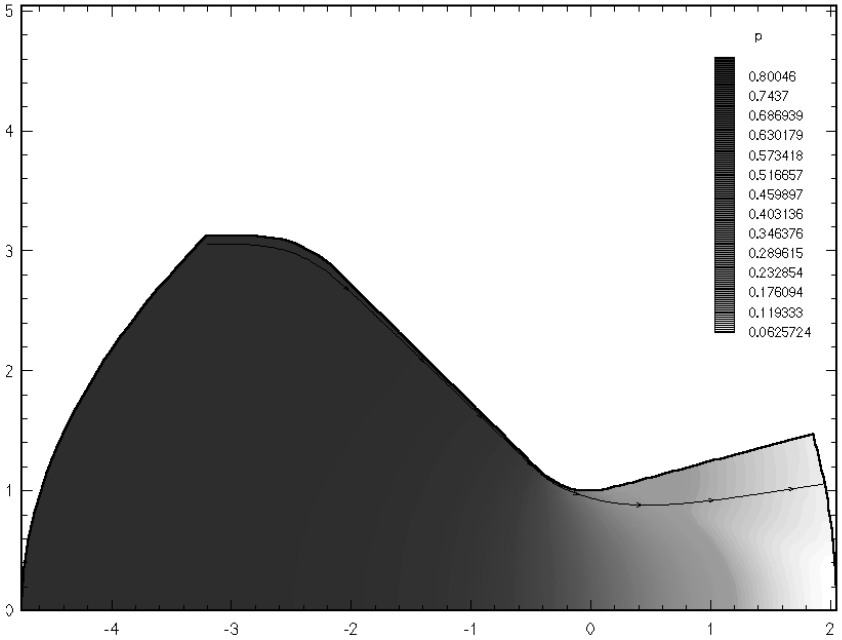

Figure 1: Gas phase pressure field in axisymmetric nozzle ($r_p = 6.0\mu m$).

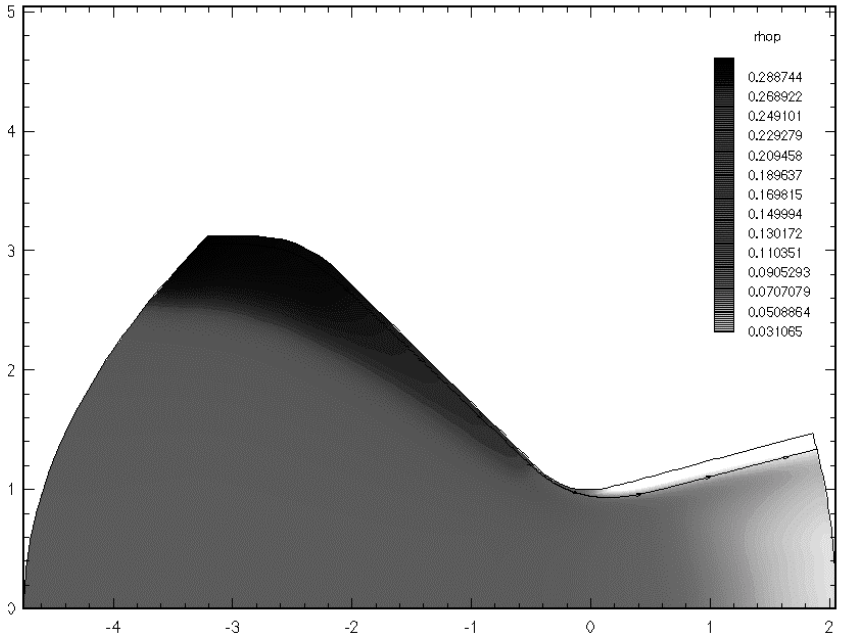

Figure 2: Particle density field in axisymmetric nozzle ($r_p = 1.0\mu m$).

Figure 1 presents the gas phase pressure contours for the case with particle radius $6.0\mu m$. Particle density contours, with particle radius $1.0\mu m$, are presented in Fig. 2. In both cases, the limiting particle streamline is also presented. In the particle density contours, the particles' behavior on the divergent portion of the nozzle shows that particles accumulate just below the limiting particle streamline. For some nozzle geometries, there is a possibility that these particles will impinge on the wall far downstream from the throat. The case of nozzle corrosion by particle impingement is discussed in detail by Ishii et al. (1987).

A comparison of the limiting streamlines achieved for various particle radii is shown in Fig. 3. As particle size increases the inertial effects are increasingly more visible and the limiting streamline moves farther away from the wall.

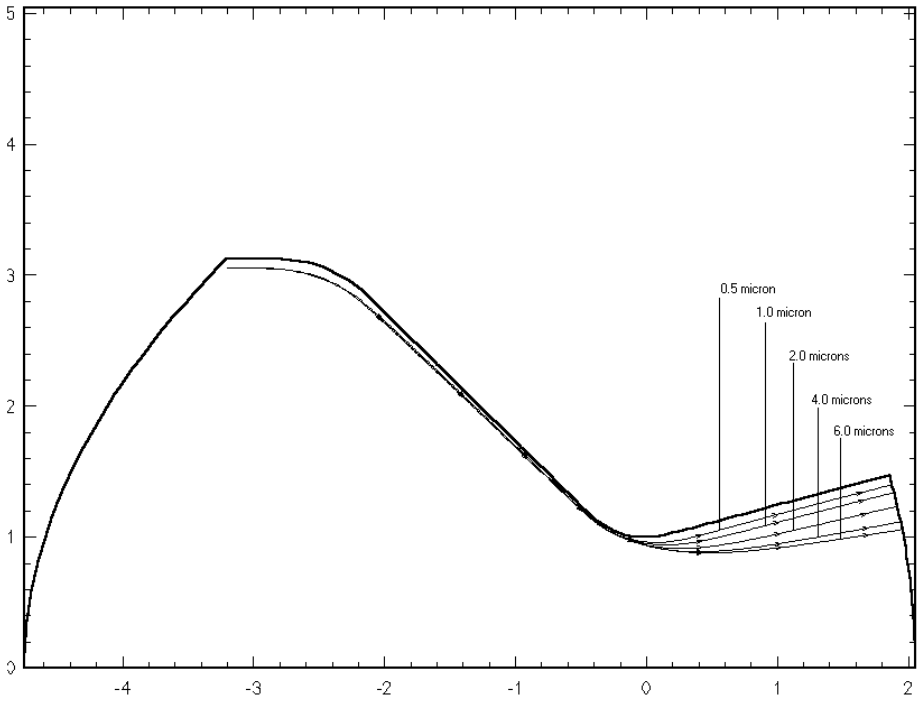

Figure 3: Limiting particle streamlines for 5 different particle radius values.

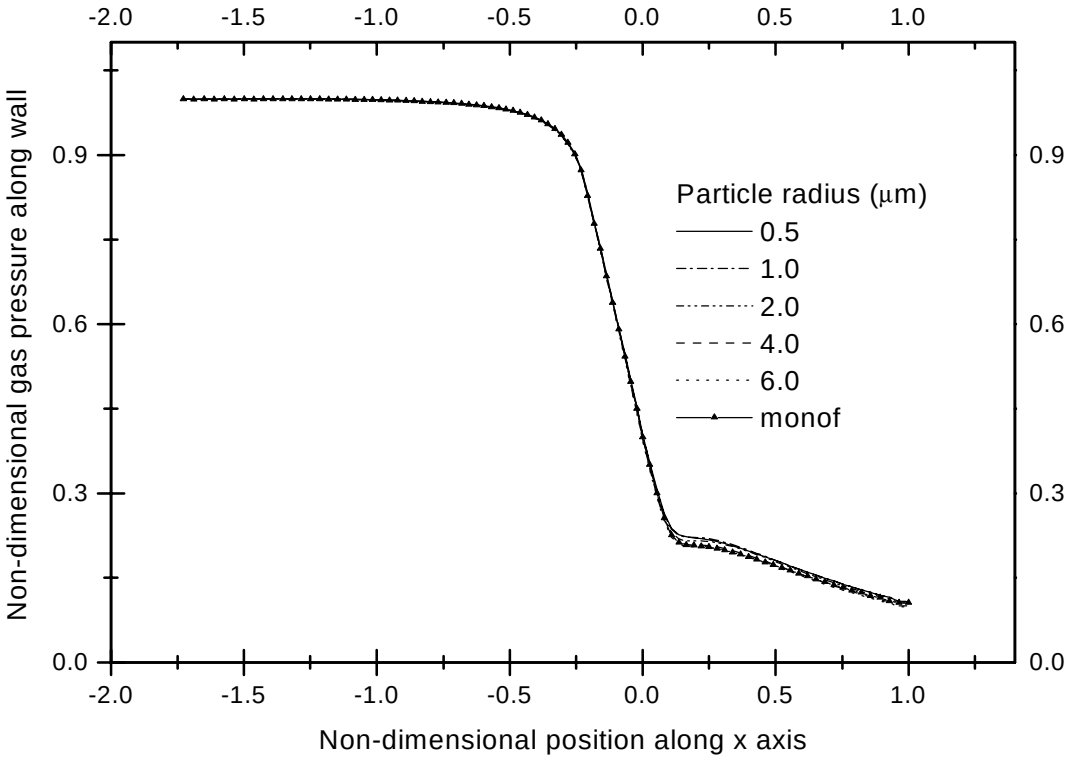

Figure 4: Dimensionless wall pressure distribution along nozzle.

Ishii et al. (1987) present experimental data from nozzles which are in agreement with Figs. 3 and 4. The largest particles that impinged on the far end of the divergent of the nozzle were smaller than 2.0 microns, which is in accordance to the results presented here. Figure 4 shows how the particle radius influences wall pressure distributions. As usual in CFD applications, it is also important to analyze the convergence characteristics of the method. The

convergence curves are presented in Fig. 5 for two different values of particle radii.

As expected, the convergence rate is slower for the larger particles. This fact is explained by the different amounts of energy which are extracted from the main flow depending on the ratio of total surface area to total volume of the particles (see Silva, 1997, for details). Thus, a two phase flow with small particles takes less time to converge than the one with larger particles.

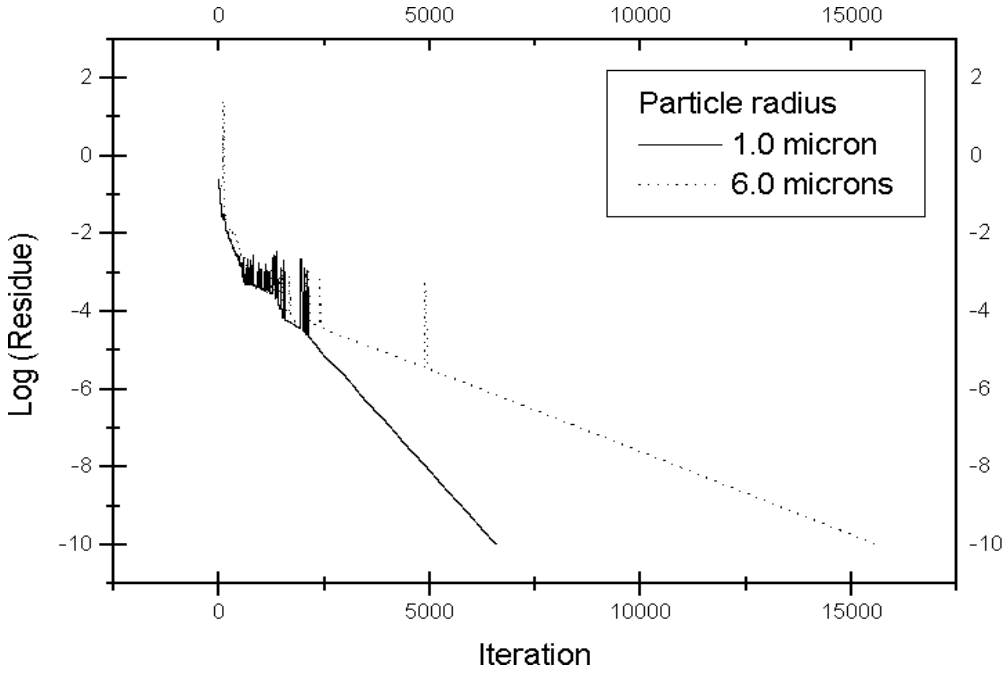

Figure 5: Typical convergence curves for the solid phase for two different radii.

5. CONCLUDING REMARKS

Axisymmetric, inviscid, two-phase nozzle flowfields were simulated using a central difference, implicit, approximated factorization algorithm. Nonlinear artificial dissipation terms were added to the right hand side Euler terms and their parameters were studied in order to maximize their effectiveness. Convergence rate was increased by the use of a spatially varying time step, thus keeping a constant CFL number throughout the flowfield. The particle and gas phases were connected by the exchange of momentum and energy, and the particles were modeled as spheres.

The validation of the code was achieved by extensively performing parametric studies on the influences of the particle radii and the two artifical dissipation coefficients as well as the CFL number. Comparing the results with available experimental and computational data, the code proved to have the expected accuracy. Gas pressure and particle density contours were compatible to the results available and were physically consistent. Mach number contours were in accordance to the work performed by Nagata (1993), and were similar to the results presented by Ishii et al. (1987) and Chang (1980, 1990).

AKNOWLEDGEMENTS

The present work was partially supported by Conselho Nacional de Pesquisa e Desenvolvimento, CNPq, under the Integrated Project Research Grant No. 522413/96-0.

REFERENCES

Azevedo, J. L. F., Fico Jr., N. G. C. R., Ortega, M. A., and Luna, G. C., 1992, Nozzle Flow Computations using the Euler Equations , Paper ICAS No. 92-4.1.2, Proceedings of the 18th Congress of the International Council of the Aeronautical Sciences, Vol. 1, Beijing, China, pp. 97-107.

Azevedo, J. L. F., Fico Jr., N. G. C. R., and Ortega, M. A., 1995, Two-Dimensional and Axisymmetric Nozzle Flow Computation Using the Euler Equations , RBCM – J. of the Braz. Soc. Mechanical Sciences, Vol. XVII, No. 2, pp.147-170.

Beam, R. M., Warming, R. F., and Hyett, B. J., 1975, Diagonalization and Simultaneous Symmetrization of the Gas Dynamics Matrices , Math Comp., Vol. 29, No. 132, pp. 1037-1045.

Beam, R. M., and Warming, R. F., 1976, An Implicit Finite-Difference Algorithm for Hyperbolic Systems in Conservation-Law Form , Journal of Computational Physics, Vol. 22, pp. 87-110.

Beam, R. M., and Warming, R. F., 1978, An Implicit Factored Scheme for the Compressible Navier-Stokes Equations , AIAA Journal, Vol. 16, No. 4, pp. 393-402.

Chang, I-S., 1980, One- and Two-Phase Nozzle Flows, AIAA Journal, Vol. 18, No. 12, pp. 1455-1461.

Chang, I-S., 1990, Three-Dimensional, Two-Phase, Transonic, Canted Nozzle Flows , AIAA Journal, Vol. 28, No. 5, pp. 790-797.

Eversole, J. D., 1984, Thermal Radiation from Carbon Particles in a Heated Nitrogen Gas Flow , Applied Optics, Vol. 23, No. 19, pp. 3439-3443.

Henderson, C. B., 1976, Drag Coefficients of Spheres in Continuum and Rarefield Flows, AIAA Journal, Vol. 14, No. 6, pp. 707-708.

Ishii, R., and Umeda, Y., 1987, Nozzle Flows of Gas-Particle Mixtures , Phys. Fluids, Vol. 30, pp 752-760.

Ishii, R., Umeda, Y., and Yuhi, M., 1989, Numerical Analysis of Gas-Particle Two-Phase Flows , Journal of Fluid Mechanics, Vol. 203, pp. 475-515.

Mehta, R.C., and Jayachandran, T., 1998, A Fast Algorithm to Solve Viscous Two-Phase Flow in an Axisymmetric Rocket Nozzle, Int. J. Numer. Meth. Fluids, Vol. 26, pp. 501-517.

Nagata, E., 1993, Numerical Analysis of Two-Dimensional, Two-Phase Flows in Transonic Convergent-Divergent Nozzles, Graduation Project, Dept. of Aeronautical Engineering, Instituto Tecnológico de Aeronáutica, São José dos Campos, SP (in Portuguese).

Novo, M.A., and Menezes, S. I., 1998, A Detailed Numerical Study of Two-Phase Flows in Rocket Motor Nozzles, Graduation Project, Dept. of Aeronautical Engineering, Instituto Tecnológico de Aeronáutica, São José dos Campos, SP (in Portuguese).

Pulliam, T.H., 1986, Artificial Dissipation Models for the Euler Equations, AIAA Journal, Vol. 24, No. 12, pp. 1931-1940.

Silva, R.P., 1997, Simulation of Two-Phase Flows in Axisymmetric Rocket Motor Nozzles, Graduation Project, Dept. of Aeronautical Engineering, Instituto Tecnológico de Aeronáutica, São José dos Campos, SP (in Portuguese).